

MODELLING OF NUCLEAR FUEL CLADDING TUBES CORROSION

MIROSLAV CECH^{a,*}, MARTIN SEVECEK^{a,b}

^a Department of Nuclear Reactors, Faculty of Nuclear Sciences and Physical Engineering, Czech Technical University in Prague, V Holesovickach 2, Praha 8, Czech Republic

^b ALVEL a.s., Opletalova 37, Praha 1, Czech Republic

* corresponding author: miroslav.cech@post.cz

ABSTRACT. This paper describes materials made of zirconium-based alloys used for nuclear fuel cladding fabrication. It is focused on corrosion problems their theoretical description and modeling in nuclear engineering.

KEYWORDS: corrosion, zirconium alloys, nuclear fuel, cladding, modelling.

1. INTRODUCTION

Tubes covering nuclear fuel in current light water reactors (LWR) are made of zirconium-based alloys since the very origin of nuclear power utilization. Zirconium-based alloys were first used in nuclear reactors of U.S. nuclear submarines. Later, Zr was adopted by fuel vendors as a suitable material for fuel cladding for commercial reactors around the world. Zirconium has been chosen for its low cross section for neutron absorption, good corrosion resistance, and other outstanding thermomechanical characteristics.

Various degradation processes jeopardizing nuclear cladding integrity take place during reactor normal operation such as grid-to-rod fretting, debris-induced failures, crud-induced localized corrosion, waterside corrosion, and hydriding. This article is focused on water corrosion, its quantification, and theoretical description. Corrosion reaction caused mainly by an interaction of nuclear fuel cladding and coolant takes place on an external surface of cladding tubes, less frequently reacts internal cladding surface with oxygen released from pellets. In case of LWRs, metal reacts with water and zirconium oxide arises:



Hydrogen released from the reaction described above partly dissolve in coolant water and partly penetrates tubes causing hydriding of zirconium. The fraction of hydrogen released from the reaction that is locally absorbed by the cladding tube is called pickup fraction and in PWR conditions is found to be constant for particular Zr-based alloys [1].

Oxygen diffuses through the zirconium oxide layer and in an interface of metal and oxide causes additional oxidation. The density of the ZrO_2 is smaller than zirconium alloy density. The difference in density and different thermal expansion of materials is the primary cause of tension, internal stresses, and strains in cladding tubes. Moreover, thermal conductivity λ of ZrO_2 is much smaller than that of zirconium based

alloys causing the Zirconium dioxide layer to decrease the heat transfer from the fuel pellet over the cladding to the coolant and consequently increase maximal temperature in the fuel pellet. The exact physical parameters depend on temperature and models of thermal conductivity of Zirconium dioxide. They are in details described in [2] and [3]. For example, the thermal conductivity of E110 alloy is about 18 W/mK at the temperature of 300 °C. The thermal conductivity of the ZrO_2 for the same temperature is only about 2 W/mK. The bulk density of the Zircaloy-4 alloy and Zirconium dioxide at the same temperature is 6.5 and 5.6 kg/m³ respectively. When the Zirconium dioxide layer thickness exceeds about 100 μm (Zircaloy-4), it might crack and it is washed away by the streaming coolant which can lead to cold spots, additional oxidation, hydridation and later cladding breach [4].

Oxidation takes place also on the internal surface of fuel cladding, where metal reacts with oxygen released from the fuel pellets where fission takes place. When a high burn-up is reached, a bonding layer consisting of ZrO_2 , UO_2 , and fission products appears. This layer might be the cause of a firm connection between the fuel cladding and pellets.

2. ZIRCONIUM BASED ALLOYS

Zirconium-based alloys has been used as the nuclear fuel cladding since 1950s [6]. There were originally two main groups of Zr-based alloys developed:

- (1.) Zirconium-Tin and Iron-based alloys (originally developed in the U.S.)
- (2.) Zirconium-Niobium based alloys (originally developed in former USSR)

During the evolution of the nuclear fuel, fuel vendors and research organizations developed dozens of concepts of fuel cladding alloys. However, the two main groups remained as can be seen in Figure 1. Different cladding concepts can be based on the figure

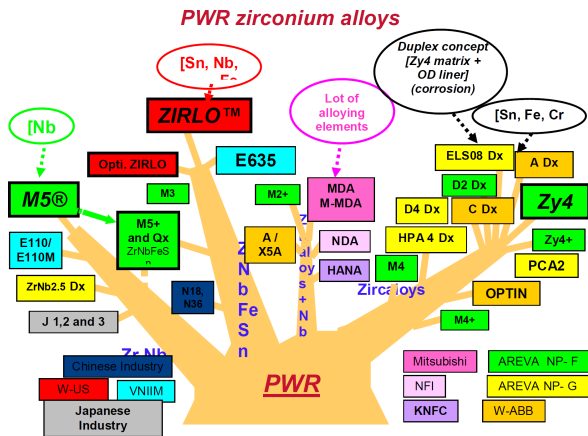


FIGURE 1. Nuclear fuel cladding alloys developed for usage in PWR reactors [5]. There were two main groups of cladding alloys developed: Zr-Sn (right branch) and Zr-Nb (left branch) based alloys with dozens other concepts depending on the alloying elements introduced around the world.

divided into four development directions depending on their composition and development history. Each alloy has a different corrosion characteristics depending on the alloying elements but also on manufacturing process and reactor type.

2.1. ZIRCONIUM-TIN ALLOYS

A well-known family of alloys called Zircaloy was developed under a Westinghouse-led program. An alloy first developed is called Zircaloy-1. This alloy was replaced by the innovative Zircaloy-2, which is still in use in the BWR reactors. After abandoning of the Zircaloy-3 alloy development and utilization due to metallurgical processing issues, concerns with the high hydrogen pickup fraction exhibited by the Zircaloy-2 alloy led to the development of the Zircaloy-4 alloy. Nickel was substituted by iron in this alloy and it was used from the 1950s to 1990s.

2.2. ZIRCONIUM-NIOBIUM ALLOYS

An alloy called E110 has been used by the Russian nuclear industry for nuclear fuel cladding fabrication for VVER reactors fuels. Similar alloys made of zirconium-doped by niobium were used from the origin of the nuclear power utilization in the USSR.

Recently, Westinghouse replaced Zircaloy-4 alloy in most of their nuclear fuel for PWRs by the ZIRLO alloy. In BWR reactors, Zircaloy-2 is still in use. ZIRLO is doped with niobium and is similar to the Russian alloy called E635. French alloy called M5 is a zirconium-based alloy containing 1% of niobium with oxygen. The M5 alloy is produced by the French company Areva since 1990s.

Generally, alloys doped with niobium such as E110, M5, and ZIRLO have a higher corrosion resistance than alloys from the Zircaloy family. Summary of composition of currently widely employed alloys is presented in Table 1 [7].

3. CORROSION MODELS

The growth and development of the cladding corrosion layer for each zirconium-based alloy is usually expressed by corrosion models.

3.1. GARZAROLLI MODELS

Models developed by Garzarolli et al. [8] are adopted for describing the thickness of the corrosion layer of cladding tubes made of Zircaloy-4, M5, and ZIRLO alloys under PWR conditions. These models generally based on Arrhenius law divide a growth of corrosion layer into two phases:

- (1.) The first phase continues until a transition thickness of oxide layer s_{tr} is reached. The rate of corrosion layer growth is expressed by the cubic rate law – Equation (2) (original units and the temperature of oxide-metal interface is used) [2, 3].
- (2.) After reaching an alloy-specific transition thickness of oxide layer s_{tr} , second phase quantified by a linear differential Equation (3) taking into account also fast neutron flux Φ is adopted.

There are other transition points observed during the corrosion process. However, only the first transition is significant for the general progress of the corrosion kinetics. For modelling purposes the use of only one transition is satisfactory. Model is defined for temperature range of 250–400 °C.

$$\frac{ds^3}{dt} = \frac{A}{s^2} \exp\left(-\frac{Q_1}{RT}\right), \quad (2)$$

$$\frac{ds}{dt} = (C_0 + U(M\Phi)^P) \exp\left(-\frac{Q_2}{RT}\right), \quad (3)$$

where

- s ... Oxide layer thickness [μm],
- T ... Temperature [$^{\circ}\text{C}$],
- Φ ... Neutron flux [$\text{neutrons}/\text{m}^2\text{s}$],
- $A = 6.3 \times 10^9 \text{ m}^3/\text{day}$,
- $R = 1.98 \text{ cal}/\text{mol K}$,
- $C_0 = 8.04 \times 10^7 \text{ } \mu\text{m}/\text{day}$,
- $M = 7.46 \times 10^{-15} \text{ cm}^2\text{s}/\text{n}$,
- $P = 0.24$,
- $U = 2.59 \times 10^8 \text{ } \mu\text{m}/\text{day}$.

Values of constants Q_1 , Q_2 and transition thickness of oxide layer s_{tr} are alloy-dependent and are summarized in Table 2 for four widely used alloys which were subject to many studies.

In literature, there were modifications of correlation models (2) and (3) defined. Modified models differ by values of constants and consider other physical phenomena neglected in the presented models. These models are implemented for example in FEMAXI and FRAPCON fuel performance codes.

Alloying element	Zircaloy-4	ZIRLO	M5	E-110	E-635
Sn	1.2–1.7 %	0.96–0.98 %			1.25–1.30 %
Fe	0.18–0.24 %	0.094–0.105 %		< 500 ppm	0.30–0.35 %
Cr	0.07–0.13 %	79–83 ppm		< 200 ppm	
Nb		1.02–1.04 %	0.8–1.2 %	0.9–1.1 %	1.0 %
Ni				0.01 %	
N	< 65 ppm	22–30 ppm		< 60 ppm	30–40 ppm
C	150–400 ppm	60–80 ppm		< 200 ppm	< 200 ppm
O	900–1400 ppm	900–1200 ppm	0.11–0.17 %	< 1000 ppm	0.07 %

TABLE 1. Composition of zirconium-based alloys widely used around the world in PWRs as materials for cladding tubes fabrication [7].

	Q_1 [cal/mol]	Q_2 [cal/mol]	s_{tr}
Zircaloy-4	32289	27354	2 μ m
M5	27446	29816	7 μ m
ZIRLO	32289	27080	2 μ m
Opt.ZIRLO	32289	27354	2 μ m

TABLE 2. Values of corrosion model's constants used in corrosion models (2) and (3) as defined by [3].

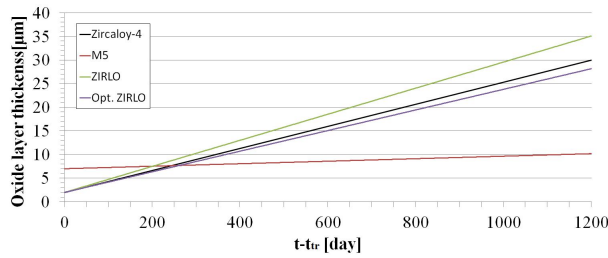


FIGURE 2. Zirconium dioxide layer development from the point of reaching first transition thickness s_{tr} corresponding to the transition time t_{tr} . Axis x represents time in days after the moment, when transition thickness was reached. The temperature of 320 °C and neutron flux of 1×10^{15} neutrons/ m^2s were chosen in this model situation.

3.2. THREE-PHASE MODEL

Another model for describing of Zircaloy-4 corrosion layer thickness in PWR conditions divides its evolution into three phases instead of two. The purpose is a faster oxide thickness growth after the second transition thickness is reached [7]. The model was developed by experimental data fitting and is more precise for higher values of oxide thickness than model developed by Garzarolli et al. [8]. Oxide layer growth during the first phase can be calculated by the following expression [6]

$$\frac{ds^3}{dt} = 2.187 \times 10^{-13} \exp\left(-\frac{135188}{RT}\right). \quad (4)$$

The first transition thickness is the same as in the previous model – 2 μ m for Zircaloy-4. Afterward,

different formula is used instead of Equation (3)

$$\frac{ds}{dt} = \left(9.31 \times 10^{-4} + 2.75 \times 10^{-3} \left(\frac{\Phi}{5.24 \times 10^{18}}\right)^{0.24}\right) \cdot \exp\left(-\frac{114526}{RT}\right). \quad (5)$$

After reaching the second transition thickness – 35 μ m, following equation is used

$$\frac{ds}{dt} = \left(9.31 \times 10^{-4} + 2.75 \times 10^{-3} \left(\frac{\Phi}{5.24 \cdot 10^{18}}\right)^{0.24}\right) \cdot 1.8 \exp\left(-\frac{114526}{RT}\right). \quad (6)$$

3.3. E110 CORROSION MODEL

A model describing the corrosion layer growth of E110 alloy in VVER conditions was developed by fitting experimental data at the Russian A.A. Bochvar High-technology Scientific Research Institute for Inorganic Materials. For the E110 alloy following relation was derived [9]

$$\frac{ds}{dt} = 40 \exp\left(-\frac{5147}{T}\right). \quad (7)$$

Model was derived by data base on experiments, which took place in temperature range of 320–360 °C. This model considers only one phase of corrosion layer development, transition thickness is disregarded. Comparison between corrosion layer growth of Zircaloy-4 and E110 is plotted in Figure 3.

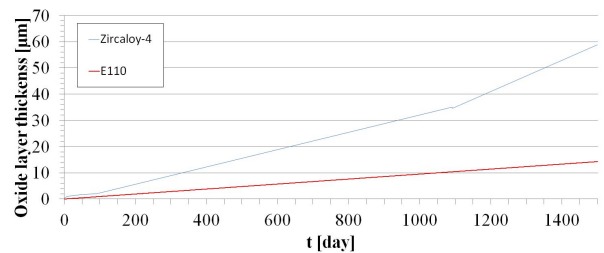


FIGURE 3. Comparison of the zirconium oxide layer thickness of Zircaloy-4 and E110 alloys in conditions of 320 °C and neutron flux of $1E15$ neutrons/ m^2s .

The corrosion growth of E110 is considerably lower in comparison with the Zircaloy-4 alloy. Accelerating

growth can be seen for the Zircaloy-4 three-phase model which is not the case for the E110 alloy. For that reason, the neglecting of transitions in case of E110 is justified.

If the behavior of nuclear fuel during LOCA, RIA or other design basis accidents is calculated by fuel performance codes like FRAPTRAN or TRANSURANUS, the thickness of oxide layer is an initial condition which strongly influences a progress of the accident and its consequences.

4. CORROSION IN LOCA CONDITIONS

Large Break Loss of Coolant Accident (LBLOCA) is the maximal design basis accident of PWRs of second and third generation. During this accident, a temperature of the whole fuel rod including pellets quickly rises due to limited cooling conditions. The high temperature of fuel pellets leads to high-temperature gradients, stresses, and cracking of pellets. Rapid release of fission gases from the fuel can be observed and the internal pressure of filling gas rises.

The high temperature of cladding together with the high internal pressure can be a cause of a deformation, ballooning, or bursting of the cladding. This geometry changes can limit the coolant flow and further reduce the heat transfer from the fuel rods to the coolant.

Construction of reactor, design of the nuclear fuel and its properties must ensure that acceptance limits for LOCA accidents will not be violated:

- (1.) A peak cladding temperature can nowhere exceed 1204 °C
- (2.) Sufficient fuel rod strength upon quench taking into account an additional mechanical load (maintain post-quench ductility)
- (3.) Fraction of zirconium reacted into oxide cannot exceed 1 % (due to hydrogen production)
- (4.) Melting temperature of fuel can not be reached in any place of the reactor core

4.1. CORROSION MODELS IN LOCA CONDITIONS

To develop corrosion models in LOCA conditions, it is necessary to measure experimental data in similar conditions. Experiments are done at high-temperature steam (800–1200 °C). Experiments with as-received cladding tubes and as well as with cladding tubes with corrosion layer has been performed. Preoxidation of experimental samples ensures that simulation will be performed in conditions which are similar to the real LOCA accident conditions with operating fuel.

A model of high-temperature corrosion of sponge based E110 alloy was developed at the UJP in the Czech Republic and is based on its experimental data [10]. Experiments cover a wide range of conditions (temperature 600–1300 °C and 0–480 minute long exposition). These wide conditions enable to use the model in various conditions and for various scenario for E110 alloy.

No.	T [°C]	Process
1	600–750	Phases $\alpha + \beta$ transformation
2	750–950	Formation of β phase
3	950–1100	Delated transformation, tetragonal oxide
4	1100–1300	Tetragonal oxide

TABLE 3. Physical processes taking place in zirconium E110 alloy in different temperature intervals during LOCA accident conditions.

This model describes a mass growth of oxide as defined in [10]

$$\Delta G = A \exp\left(\frac{E}{T}\right) t^n = kt^n, \quad (8)$$

where

ΔG ... mass growth [mg/dm²],

A, E, k ... fitting parameters,

t ... time [s],

n ... kinetic constant.

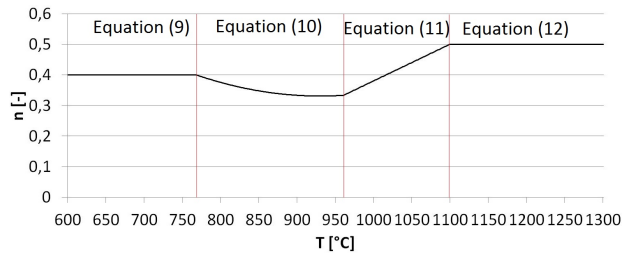


FIGURE 4. Development of the parameter n with temperature as defined by [10].

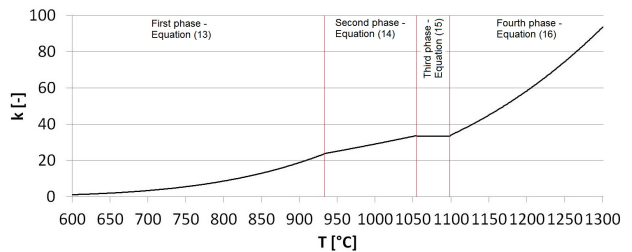


FIGURE 5. Development of the parameter k with temperature as defined by [10].

For n and k parameters were derived following formulas

$$n = 0.4 \quad \text{for } T < 768.4 \text{ °C} \quad (9)$$

$$n = 2.609 - 4.898 \times 10^{-3}(T - 273.15) + 2.633 \times 10^{-6}(T - 273.15)^2 \quad \text{for } T < 960.3 \text{ °C} \quad (10)$$

$$n = 1.202 \times 10^{-3}(T - 273.15) - 0.8208 \quad \text{for } T < 1098.9 \text{ °C} \quad (11)$$

$$n = 0.5 \quad \text{for } T > 1098.9 \text{ °C} \quad (12)$$

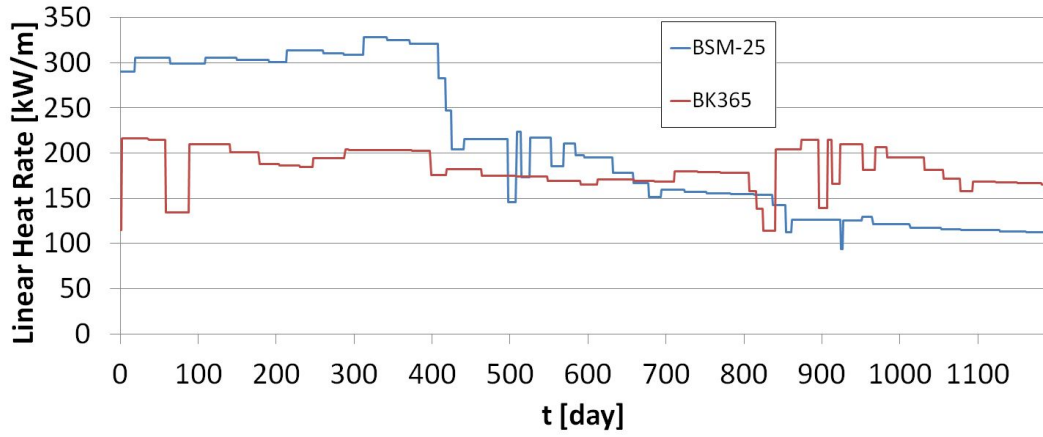


FIGURE 6. Power history of rods BSM-25 and BK365.

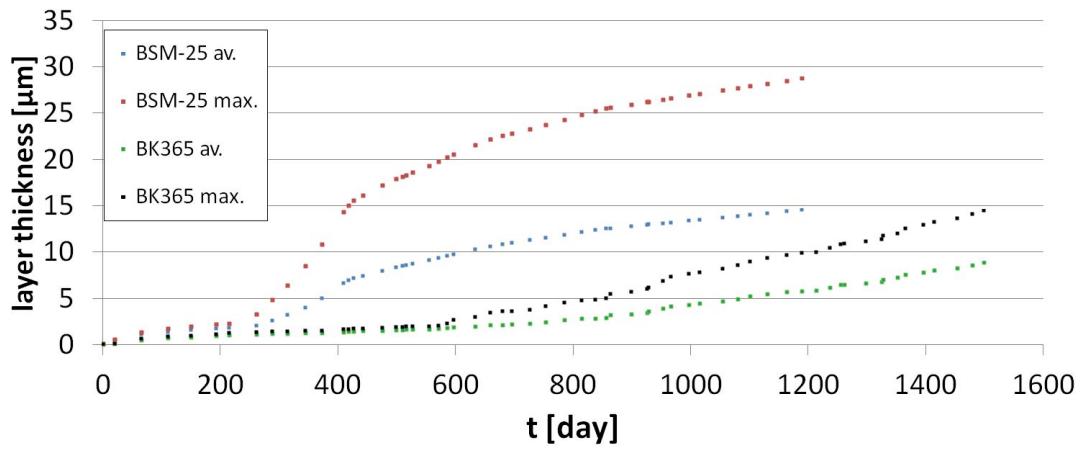


FIGURE 7. Oxide layer thickness of BSM-25 and BK365 rods.

$$k = 85265.6 \exp\left(-\frac{9875.59}{T}\right) \quad \text{for } T < 934.1^\circ\text{C} \quad (13)$$

$$k = 1072.21 \exp\left(-\frac{4592.6}{T}\right) \quad \text{for } T < 1054.5^\circ\text{C} \quad (14)$$

$$k = 33.33 \quad \text{for } T < 1098.0^\circ\text{C} \quad (15)$$

$$k = 96482.3 \exp\left(-\frac{10913.1}{T}\right) \quad \text{for } T > 1098.0^\circ\text{C} \quad (16)$$

Temperature intervals of equations (9)–(16) approximately correspond to physical processes, which take place in the cladding material during LOCA accident. These processes are described in Table 3.

This model well describes a corrosion kinetic for all ranges of temperature covered by experiment. The value of parameter n is $1/2$ for high-temperature corrosion and $1/3$ for middle-temperature corrosion [7]. These values are the same as in other used models. Another model for n also very well describes the n temperature reliance.

Constant k equals approximately equals to 0 and increase with temperature to about 90 at 1300°C . Di-

viding model into four ranges where different formulas are used brings a good agreement of the model with experimental data. A comparison between this model and data can be found in [10].

5. MODEL OF CORROSION IN FEMAXI

A calculation of oxide layer development in the FEMAXI-6 code has been performed for two fuel rods: BSM-25, and BK365. These rods were irradiated in the BR-3 reactor and reached burn-up of 66 and 52 MWd/kgHM. Rods were irradiated within the High Burnup Effect Program in the BR-3 reactor, cladding was made of Zircaloy-4 alloy, coolant inlet temperature was 255°C .

A model originally developed by Garzarolli et al. [8] (Equations (2) and (3)) was used for the Zircaloy-4 alloy corrosion modeling. The two power histories used as a model input are plotted in Figure 6. Corresponding oxide layer thickness growth is shown in Figure 7. For both tested fuel rods, an average thickness and the maximal oxide layer thickness are shown. Maximal thickness of the corrosion layer is about two times higher than the average value. Maximal thickness was reached in the middle of the fuel rod which does

not correspond to the case in commercial power reactors. The oxide layer growth is strongly dependent on the temperature, the higher the temperature is the faster the growth. Therefore, the maximal thickness of the zirconium oxide layer in commercial power reactors is at the top of the fuel rod where the coolant temperature is highest.

Figure 7 shows, that higher linear heat rate causes faster oxide layer creation. The graph also shows that the first phase of oxide layer growth is independent of fast neutron flux. Small differences are caused by higher temperature. In the later phase of fuel rod's irradiation, there is a clear dependance of corrosion layer thickness on fast neutron flux and linear heat rate. When BSM-25 rod was operating in high heat rate condition, layer growth was much faster than in the case of smaller heat rate of the second fuel rod. Higher heat rate (and corresponding temperature) causes the bigger corrosion layer, even when the burnup of the BSM-25 rod is lower.

6. CONCLUSION

This article describes models quantifying corrosion of nuclear fuel cladding tubes made of zirconium-based alloys widely used in nuclear industry in nominal conditions and LOCA accident conditions. Models used for calculating of an oxide layer thickness in normal operation conditions for the widely used alloys Zircaloy-4, ZIRLO, M5 and E110 are presented and compared. A model for corrosion and high-temperature oxidation in LOCA conditions is described and reliance of particular parameters used in models are shown in graphs. A corrosion model for nominal conditions was applied in the FEMAXI-6 code to calculate corrosion of fuel rods BK363 and BSM-25 tested in the BR-3 reactor. The relations of burnup, linear heat rate, and corrosion layer thickness growth is illustrated in the example. Results show faster oxide growth in case of BSM-25 rod after reaching the transition thickness for Zircaloy-4 alloy, because this rod was operated at higher linear heat rate.

ACKNOWLEDGEMENTS

This work was supported by the Grant Agency of the Czech Technical University in Prague, grant No. SGS OHK4-008/16.

REFERENCES

- [1] K. Geelhood, W. Luscher. Frapcon-3.5: Integral assessment. *Progress in Nuclear Energy* 2014.
- [2] M. Suzuki, H. Saitou, N. G. K. K. Kikō. *Light Water Reactor Fuel Analysis Code: FEMAXI-6 (Ver. 1): Detailed Structure and User's Manual*. Japan Atomic Energy Research Institute, 1997.
- [3] W. G. Luscher, K. J. Geelhood, et al. *Material property correlations: comparisons between FRAPCON-3.4, FRAPTRAN 1.4, and MATPRO*. US Nuclear Regulatory Commission, Office of Nuclear Regulatory Research, 2011.
- [4] P. Billot, B. Cox, K. Ishigure, et al. Corrosion of zirconium alloys in nuclear power plants. In *TECDOC-684*. International Atomic Energy Agency (IAEA), 1993.
- [5] L. Hallstadius, S. Johnson, E. Lahoda. Cladding for high performance fuel. *Progress in Nuclear Energy* **57**:71–76, 2012.
- [6] A. T. Motta, A. Couet, R. J. Comstock. Corrosion of zirconium alloys used for nuclear fuel cladding. *Annual Review of Materials Research* **45**:311–343, 2015.
- [7] D. Kobyłka. Termofyzikální vlastnosti pokrytí nových typů paliva, jejich implementace v kódu FEMAXI-6 a testování. Tech. Rep. 14117/2012/02Kob, ÚJV Řež, a.s., 2012.
- [8] F. Garzarolli, D. Jorde, R. Manzel, et al. Review of PWR fuel rod waterside corrosion behavior. Tech. rep., Kraftwerk Union AG, Erlangen (Germany, FR); Combustion Engineering, Inc., Windsor, CT (USA), 1980.
- [9] V. Konkov, M. Sablin, T. Khokhunova, et al. Assessment of E110 and E635 alloy corrosion behavior in VVER-1200 reactors. *JSC VNIINM* 2009.
- [10] J. Krejčí. Oxidace palivového pokrytí během havárie LOCA. *Bezpečnost jaderné energie* **45**:311–343, 2015.